



## A DESIGN AND SIMULATION STUDY OF ZERO-IF GILBERT-CELL MIXER FOR WIMAX RECEIVERS

Frederick Ray I. Gomez

\* New Product Introduction Department, Back-End Manufacturing & Technology, STMicroelectronics, Inc. 9 Mountain Drive, Light Industry & Science Park II, Brgy. La Mesa, Calamba City, Laguna, Philippines 4027

DOI: 10.5281/zenodo.1745378

**KEYWORDS:** Gilbert-cell mixer; double-balanced mixer; zero-IF; WiMAX; conversion gain; noise figure.

### ABSTRACT

Differential approach is becoming highly preferred in RFIC (radio frequency integrated circuit) design due to its advantages, particularly its high immunity to common-mode noises, satisfactory rejection of parasitic coupling, and increased dynamic range. One particular RF front-end building block that is often designed as differential circuit is the mixer. This paper presents a study and design of a differential mixer, particularly the Gilbert-cell or double-balanced mixer implemented on a zero-IF (zero-intermediate frequency) or direct-conversion architecture in a standard 90nm CMOS (complementary metal-oxide semiconductor) process operating at frequency of 5GHz, which is a typical frequency for WiMAX (worldwide interoperability for microwave access) receiver. Impedance matching was necessary to fully optimize the mixer design. The zero-IF Gilbert-cell mixer design achieved conversion gain of 11.46dB and noise figure of 16.53dB, comparable to other mixer designs.

### INTRODUCTION

Receiver front-end of an RF (radio frequency) system is of particular interest to many designers and researchers as it proves to be the most critical part in many communication systems and wireless applications such as WiFi (wireless fidelity), Bluetooth, and WiMAX (worldwide interoperability for microwave access). The block diagram of a typical receiver is shown in Fig. 1.

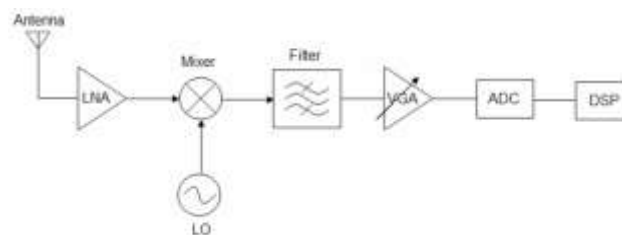


Fig. 1. Block diagram of a typical receiver.

Mixer is one of the key front-end building blocks in an RF receiver. It is also called a converter because it converts RF signals into a lower intermediate frequency (IF) by mixing with an offset local oscillator (LO). Depending on the receiver requirements, mixers must undergo a careful design process since a lot of tradeoffs among different performance parameters must be considered and understood. Ultimately, the objective is to study and design a zero-IF Gilbert-cell mixer implemented in a standard 90nm Complementary Metal-Oxide Semiconductor (CMOS) process. Operating frequency is set to 5GHz, which is a typical frequency for a WiMAX receiver.

### REVIEW OF RELATED LITERATURE

RF receivers can be categorized as superheterodyne (high-IF), low-IF, and zero-IF or homodyne or direct-conversion based on the resulting IF signal they operate. For the zero-IF receiver, IF is designed to be centered at frequency zero, meaning the LO frequency is equal to the input RF frequency. Image signal is avoided and the analog filtering problem can be easily handled. With zero IF, the desired signal is translated directly to the baseband, allowing analog-to-digital converter (ADC) and digital signal processing (DSP) circuits to perform modulation and other ancillary functions [1] [2]. This eliminates the need for highly complex filters since channel selection only requires a low-pass filter (LPF) as shown in Fig. 2 with sharp



cutoff characteristics, and thus allowing the possibility of monolithic integration. With this, smaller and cheaper receivers with low power consumption may be realized for various wireless applications like Bluetooth, WiFi, and WiMAX. Many of the implemented receivers in WiMAX [3] [4] [5] use the zero-IF architecture since the LPFs make sure that the closely-spaced carrier signals do not cause interference with each other.

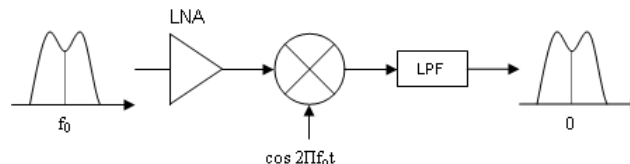


Fig. 2. Zero-IF receiver.

Designing a mixer must take into account the many trade-offs among the performance parameters. Thus, a careful study of these important parameters must be done in order to design fully-functional mixers. A mixer's efficiency on frequency conversion from RF to IF is characterized by conversion loss or gain. It is the ratio of the desired IF output to the value of the RF input. Conversion gain ( $CG$ ) may be expressed in voltage or power. In cases when the conversion gain is less than unity or 0dB, it is aptly termed as a conversion loss.

$$CG_{voltage} = 20 \log \frac{V_{IF}}{V_{RF}} \quad \text{Eq. (1)}$$

$$CG_{power} = 20 \log \frac{P_{IF}}{P_{RF}} \quad \text{Eq. (2)}$$

$V_{IF}$  and  $V_{RF}$  are the root mean square (RMS) voltages of the IF and RF signals, respectively, while  $P_{IF}$  and  $P_{RF}$  are the equivalent power of the IF and RF signals, respectively. Conversion gain is preferred over conversion loss because of the benefit of amplification along with frequency translation. However, it should be noted that conversion gain directly affects the noise figure and linearity of the overall receiver. Hence, design tradeoffs concerning these parameters are inevitable.

Another important mixer parameter is the noise figure ( $NF$ ). It is a measure of the amount of signal-to-noise-ratio ( $SNR$ ) degradation introduced by the mixer as seen at the output. Eq. 3 shows the relation between the  $SNR$  at the input port and the  $SNR$  at the output port of the mixer, often expressed in dB.

$$NF = 10 \log \left( \frac{SNR_{IN}}{SNR_{OUT}} \right) \quad \text{Eq. (3)}$$

Noise figures of mixers tend to be higher than amplifiers (e.g. low-noise amplifiers, power amplifiers) because of the contribution of noise from other frequencies (apart from input RF signal) that can mix down to the IF. This considerable noise in mixers is the main reason why low-noise amplifiers (LNA) are used in the front-end of a receiver [6].

The selection of mixer architecture depends on the application and the requirements for the different design parameters. The dynamic range of most RF receivers is often limited by the first down-conversion mixer. This leads to many tradeoffs among the performance parameters such as conversion gain, noise figure, linearity and isolation. Integrated mixers are preferred over their discrete counterparts because they can offer high level integration with cost, area, and power savings [7].

Nowadays, the most popular solution for the mixer is based on the double-balanced topology. It operates with differential LO and RF inputs. In this topology, LO products are prevented from getting to the output by combining two single-balanced mixers. As shown in Fig. 3, the two single-balanced mixers are connected in anti-parallel as far as the LO is concerned, but in parallel for the RF signal. Thus, the LO terms sum to zero in the output, whereas the converted RF signal is doubled in the output [6]. This is most desirable for high port-to-port isolation and spurious output rejection applications.

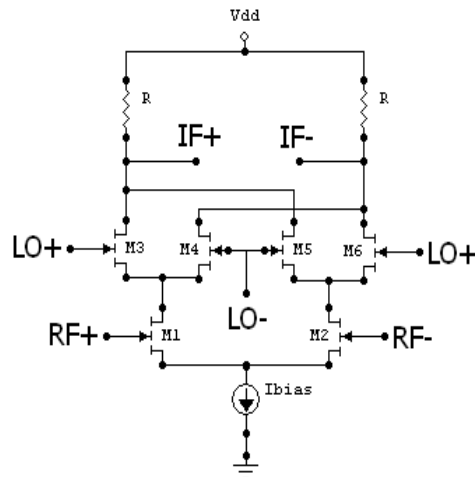


Fig. 3. Gilbert-cell or double-balanced mixer.

As earlier mentioned, the goal of the paper is to study and design a zero-IF Gilbert-cell or double-balanced mixer implemented in a standard 90nm CMOS process, operating at frequency of 5GHz which is a typical frequency for a WiMAX receiver. The target specifications of the figures of merit are based on the performance comparison in terms of conversion gain and noise figure of past researches on direct-conversion active mixer topologies given in Table 1.

TABLE I. PERFORMANCE COMPARISON

Paper	RF (GHz)	Conversion Gain (dB)	Noise Figure (dB)	Topology
[4]	2~11	21.5~22.8	21.5~25.8	Double-balanced
[5]	3.4~3.85	10	10	Single-balanced
[9]	2	19.5	10.2	BiCMOS Double-balanced
[10]	20~40	16	--	BiCMOS Single-balanced
[11]	5.2	9.3	10.5	Double-balanced

## DESIGN OF MIXER

The topology of Gilbert-cell mixer can provide high conversion gain, very low noise figure, and high degree of LO-IF isolation. The main disadvantage of this topology is its physical implementation. A balun transformer is required to convert the single-ended input to a differential RF input signal of the mixer. Transformers with very low insertion loss are difficult to realize in monolithic integration, hence this forces the use of an off-chip transformer which occupies more board space and cost [8].

It is of high importance to determine the proper biasing and sizing of all the transistors such that RF transistors (M1-M2) will operate in the saturation region while the LO transistors (M3-M6) operate near the boundary of the saturation and linear regions. The mixer design used *nsvt* (NMOS standard Vt) which is the typical model for the transistor. Shown in Fig. 4 is the schematic design of the Gilbert-cell mixer.

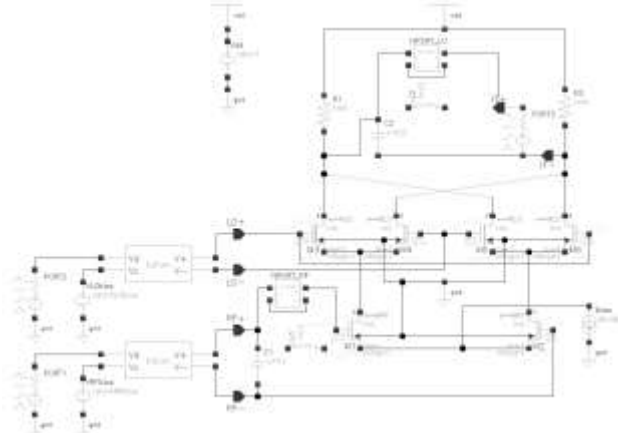


Fig. 4. Schematic design of Gilbert-cell mixer.

One way to increase the performance of the mixer in terms of conversion gain and noise figure is to apply impedance matching in the circuit.  $Z_{11}$  and  $Z_{22}$  can be obtained using *sp*-analysis which is swept from  $f_1 = 700\text{MHz}$  to  $f_2 = 6\text{GHz}$ . Actual inductor and capacitor values at  $f = 5\text{GHz}$  can be computed from the L-network reactances.

To supply differential LO input to the mixer, a port *PORT2* with a matching resistor (set to  $50\Omega$ ) is used which is then fed into an ideal passive balun to convert the single-ended signal into differential. For the differential RF input of the mixer, same setup as the LO is used with *PORT1*. To use the differential output for measurements, matching the IF output port *PORT3* to the output impedance of the mixer is necessary. *PORT1* is set to DC source type with *pacmag* (*periodic ac magnitude*) set to 1. *PORT3*, which is the IF port, is set also to DC source type. The only large signal is from *PORT2* which is a sine wave with  $f_{lo}=5\text{GHz}$  and  $P_{LO} = 0\text{dBm}$ .

For the impedance matching, the input matching network is applied before the differential RF input of the mixer instead of placing it before the balun. This will result to an adjustment on the value of  $L_1$ , which will decrease, since the balun circuit has self-inductance. The adjusted value of  $L_1$  can be determined using the *sp*-analysis swept from  $f_1 = 700\text{MHz}$  to  $f_2 = 6\text{GHz}$ . Moreover, inductors with small inductances are more realizable in actual designs than their larger counterparts. The final values of the L-matching network are summarized in Table II.

TABLE II. FINAL VALUES OF L-NETWORK ELEMENTS

L and C	Value
$L_1$	12.7nH
$C_1$	1.116087pF
$L_2$	1.328515nH
$C_2$	267.127fF

*ASITIC* (analysis and simulation of spiral inductors and transformers for ICs) [12] [13] and *SpiralCalc* (integrated spiral inductor calculator) [14] [15] are used for the design of the inductors. Table III shows the design parameters obtained for the design of the spiral inductors using *ASITIC* while Table IV shows that of using *SpiralCalc*.

TABLE III. INDUCTOR DESIGN USING ASITIC

Parameters	Inductors	
	$L_1$	$L_2$
Desired L	12.7nH	1.328515nH
No. of sides	4	8



Length, D	300 $\mu\text{m}$	190 $\mu\text{m}$
Metal width, W	10.886 $\mu\text{m}$	10.901775 $\mu\text{m}$
Spacing, S	1	1
No. of turns, N	4.25	2.5
Metal layer	7	7
Inductance, L	12.711454nH	1.328515nH
Q-factor, Q	2.32165	5.693986

TABLE IV. INDUCTOR DESIGN USING SPIRALCALC

Parameters	Inductors	
	$L_1$	$L_2$
Desired L	12.7nH	1.328515nH
No. of sides	4	8
Length, D	300 $\mu\text{m}$	190 $\mu\text{m}$
Metal width, W	11.2 $\mu\text{m}$	10 $\mu\text{m}$
Spacing, S	1	1
No. of turns, N	6	2
Inductance, L:		
Modified Wheeler	12.885 $\mu\text{m}$	1.326 $\mu\text{m}$
Current Sheet	12.739 $\mu\text{m}$	1.326 $\mu\text{m}$
Monomial Fit	12.624 $\mu\text{m}$	1.394 $\mu\text{m}$

In *ASITIC*, the spiral inductors are designed such that desired inductances are achieved and the Q-factors are optimized with eddy-current option enabled to include the effects of substrate induced eddy current losses.  $L_1$  have smaller Q-factor than  $L_2$  because of its high inductance value. For the inductor design using *SpiralCalc*, same parameter values from the *ASITIC* parameters are used except for the metal width and the number of turns of the spiral inductor. These parameters are tweaked such that the desired inductances are achieved for the inductors.

The *n2port* from the *analogLib* library is used as a model block for all the *ASITIC* inductors. *Touchstone* format of S-parameter file is used as file input of the *n2port* component since the actual S-parameters using *ASITIC* are given in *touchstone* format. The figures of merit such as conversion gain and noise figure are determined using *SpectreRF* in the *Analog Design Environment*.

## DISCUSSION OF RESULTS

A Gilbert-cell mixer's frequency converting action is characterized by conversion gain or loss. Voltage conversion gain is the ratio of the RMS voltages of the IF and RF signals. The formulae for conversion gain are also given in Eq. (1). The variations of conversion gain with the power of LO signal ( $P_{LO}$ ) can be measured using *swept PSS (Periodic Steady-State) analysis* with *PAC (Periodic AC) analysis*. The *PAC analysis* will then compute the voltage conversion gain in dB20 of the whole circuit with *PORT3* as the output port (with output harmonic of 0, which is 5GHz) and *PORT1* as the input port (with input harmonic of -1, which is 0GHz). Setting the input port to RF+ port, which is located after the balun circuit, will compute the voltage conversion gain of the mixer only. Simulation plots of the conversion gain swept from  $P_{LO} = -10\text{dBm}$  to  $P_{LO} = 30\text{dBm}$  are shown in Fig. 5-7.

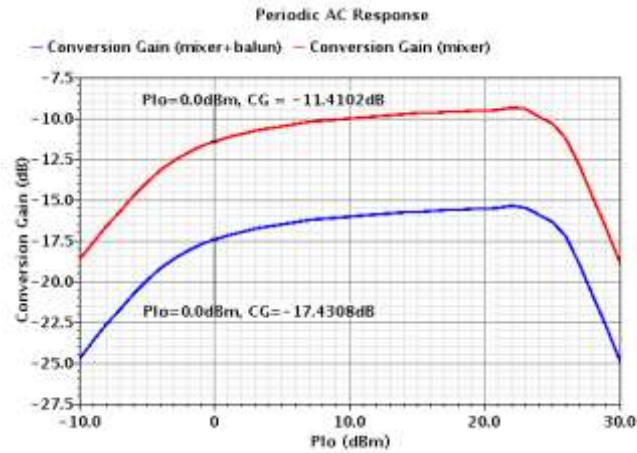


Fig. 5. Conversion gain (in dB) vs.  $P_{LO}$  of Design2 (w/o matching).

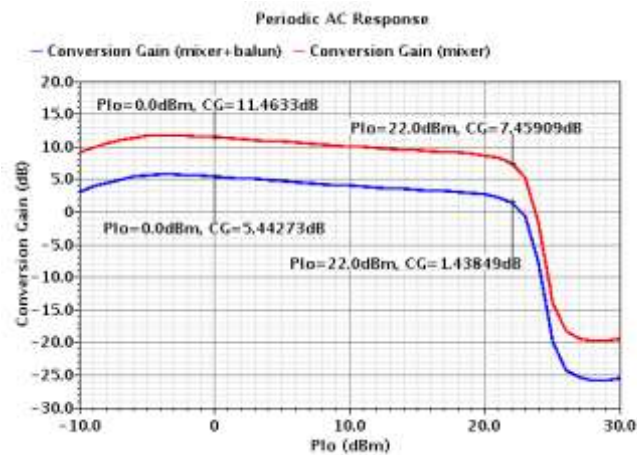


Fig. 6. Conversion gain (in dB) vs.  $P_{LO}$  of Design2 (ideal L).

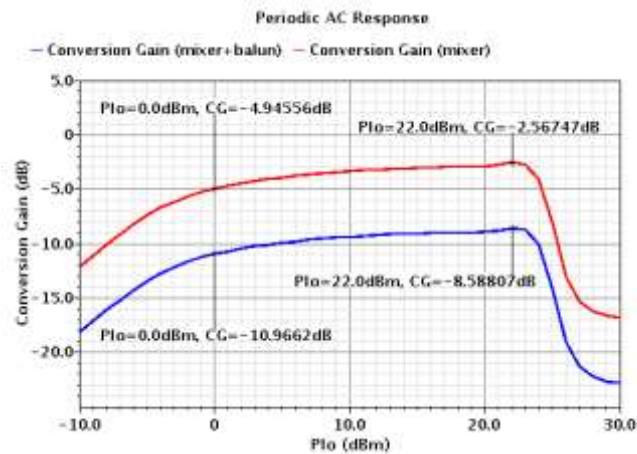


Fig. 7. Conversion gain (in dB) vs.  $P_{LO}$  of Design2 (ASITIC L).





## Global Journal of Engineering Science and Research Management

Based on the conversion gain simulation results, input and output impedance matching contribute to better conversion gain performance. Moreover, using ideal inductors for impedance matching produced better performance as compared to using non-ideal ASITIC inductors through the n2port. It can be observed from the simulation plots that the conversion gain of the mixer only is higher than the conversion gain of the whole circuit consisting of the mixer and the balun. This is because the balun in the circuit, which is a passive balun, has insertion loss and thus incapable of producing gain. When a passive balun is cascaded with another block, the overall gain is degraded.

For the noise figure, *Pnoise* (Periodic Noise) analysis with *PSS* analysis is used. In addition, *PSP* (Periodic S-Parameters) analysis with *PSS* analysis can also be used to determine the noise figure of the circuit. Noise figure from a sweep range of -10dBm to 30dBm can now be determined and plotted using these analyses. The plots are shown in Fig. 8-9.

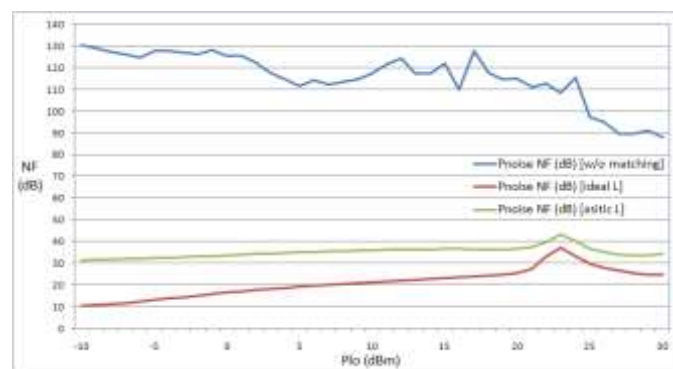


Fig. 8. Noise figure (in dB) vs.  $P_{LO}$  of Design2 (*Pnoise* analysis).

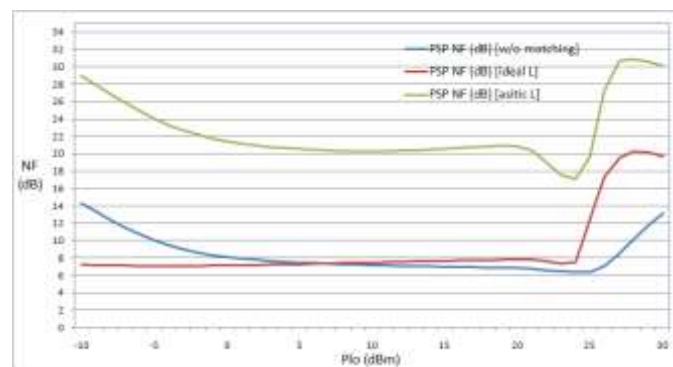


Fig. 9. Noise figure (in dB) vs.  $P_{LO}$  of Design2 (*PSP* analysis).

Input and output impedance matching also contribute to better noise performance of the circuit, as indicated in Fig. 8-9. It can be observed that using ideal inductors for impedance matching produced lower noise figure as compared to using non-ideal ASITIC inductors through the n2port model. The model block n2port introduces noise to the system, hence, adding to the total noise figure of the circuit. Table V shows a summary of simulation results for conversion gain and noise figure at  $P_{LO} = 0$ dBm.

TABLE V. SUMMARY OF SIMULATION RESULTS (AT  $P_{LO} = 0$ )

Figures of Merit	Value
<i>CG</i> (mixer+balun) [w/o matching]	-17.4308dB
<i>CG</i> (mixer) [w/o matching]	-11.4102dB
<i>CG</i> (mixer+balun) [ideal L]	5.44273dB
<i>CG</i> (mixer) [ideal L]	11.4633dB
<i>CG</i> (mixer+balun) [ASITIC L]	-10.9662dB
<i>CG</i> (mixer) [ASITIC L]	-4.94556dB
<i>Pnoise NF</i> [w/o matching]	125.355dB
<i>Pnoise NF</i> [ideal L]	16.5290dB
<i>Pnoise NF</i> [ASITIC L]	33.7129dB
<i>PSP NF</i> [w/o matching]	8.1267dB
<i>PSP NF</i> [ideal L]	7.1364dB
<i>PSP NF</i> [ASITIC L]	21.4372dB

It is evident that input and output impedance matching contribute to better performance based on the figures of merit presented for the Gilbert-cell mixer design. It is observed that the conversion gain of the zero-IF Gilbert-cell mixer is higher than the conversion gain of the circuit consisting of the mixer and the balun. The reason is that the conversion gain performance at the system-level perspective is greatly influenced by the performance of the initial or preceding blocks, for this case the passive balun. Henceforth, it is of high importance to consider the contribution of the input or previous circuit (and as well as the output or succeeding circuit) in studying and designing the mixer.

## CONCLUSIONS AND RECOMMENDATIONS

A design of zero-IF Gilbert-cell mixer was implemented and optimized on this study. Proper biasing and sizing of all the transistors were necessary to ensure the required mode of operation for all the transistors. Conversion gain and noise figure were determined to measure the mixer's performance. These performance parameters can be greatly enhanced by applying impedance matching in the circuit. The effect of the passive balun was also presented, showing the decrease in the conversion gain of the overall circuit. Ultimately, the zero-IF Gilbert-cell mixer design achieved conversion gain of 11.46dB and noise figure of 16.53dB (using *Pnoise* analysis) at 5GHz, comparable to other mixer designs from past researches.

For future studies, an active balun can be used instead of passive balun for monolithic design and implementation. Active baluns are capable of producing gain and if cascaded in a Gilbert-cell mixer to supply the differential RF and LO inputs, the overall performance of the mixer can be improved. Although active baluns are unidirectional converters, they are also used for their large bandwidth, which is beyond what non-ideal passive baluns can provide.

## ACKNOWLEDGMENT

The author would like to express appreciation to Prof. Maria Theresa De Leon, Ph.D. of Microelectronics and Microprocessors Laboratory at University of the Philippines for the technical support during the course of the study, and to the STMicroelectronics Calamba NPI Team and the Management Team for the extended support.

## REFERENCES

1. B. Razavi, "RF microelectronics," Upper Saddle River, New Jersey, USA: Prentice Hall Press, 1998.
2. W. Namgoong and T. Meng, "Direct-conversion RF receiver design," *IEEE Transactions on Communications*, vol. 49, no. 3, March 2001.
3. Y. Zhou, C.P. Yoong, L.S. Weng, Y.J. Khoi, M.C.Y. Wah, K.A.C. Moy, and D.W.T. Fatt, "A 5 GHz dual-mode WiMAX/WLAN direct-conversion receiver," *IEEE International Symposium on Circuits and Systems*, May 2006.





## Global Journal of Engineering Science and Research Management

4. J.Y. Lyu and Z.M. Lin, "A 2~11 GHz direct-conversion mixer for WiMAX applications," *IEEE Region 10 Conference*, pp. 1-4, Oct. 2007.
5. J.G. Atallah, S. Rodriguez, L.R. Zeng, and M. Ismail, "A direct conversion WiMAX RF receiver front-end in CMOS technology," *International Symposium on Signals, Circuits and Systems*, vol. 1, July 2007.
6. T. Lee, "The design of CMOS radio-frequency integrated circuits," Cambridge: Cambridge University Press, 1998.
7. G. Watanabe, H. Lau, and J. Schoepf, "Integrated mixer design," Motorola Inc., Semiconductor Products Sector, Arizona, USA.
8. M. Voltti, T. Koivisto, and E. Tiiliharju, "Comparison of active and passive mixers," *18th European Conference on Circuit Theory and Design*, pp. 890-893, August 2007
9. T. Tikka, J. Ryyanen, M. Hotti, and K. Halonen, "Design of a high linearity mixer for direct-conversion base-station receiver," in *Proc. IEEE International Symposium on Circuits and Systems*, 2006.
10. K.W. Hamed, A.P. Freundorfer, and Y.M.M. Antar, "A monolithic double-balanced direct conversion mixer with an integrated wideband passive balun," *IEEE Journal of Solid-State Circuits*, vol. 40, no. 3, March 2005.
11. J. Park, C-H. Lee, B-S. Kim, and J. Laskar, "Design and analysis of low flicker-noise CMOS mixers for direct-conversion receivers," *IEEE Transactions on Microwave Theory and Techniques*, vol. 54, no. 12, December 2006.
12. A.M. Niknejad and R.G. Meyer, "Analysis and optimization of monolithic inductors and transformers for RF ICs," in *Proc. Custom Integrated Circuits Conference*, Santa Clara, CA, pp. 375-378, May 1997.
13. A.M. Niknejad and R.G. Meyer, "ASITIC for Windows NT/2000," *Research in RFIC Design*, [http://rfic.eecs.berkeley.edu/~niknejad/Asitic/grackle/cygwin\\_info.html](http://rfic.eecs.berkeley.edu/~niknejad/Asitic/grackle/cygwin_info.html).
14. Stanford Microwave Integrated Circuits Laboratory. *Integrated Spiral Inductor Calculator*, <http://www-smirc.stanford.edu/spiralCalc.html>.
15. S.S. Mohan, M. Hershenson, S.P. Boyd and T.H. Lee, "Simple accurate expressions for planar spiral inductances," *IEEE Journal of Solid-State Circuits*, pp. 1419-1424, October 1999.